$[(\eta\text{-}C_5H_4R)Fe(CO)_2X]$, X = Cl, Br, I, NO_3, CO_2Me and $[(\eta\text{-}C_5H_4R)Fe(CO)_3]^+$, R = $(CH_2)_nCO_2Me$ (n = 0–2), and $CO_2CH_2CH_2OH$: a new group of CO-releasing molecules†‡§

David Scapens,[a] Harry Adams,[a] Tony R. Johnson,[a] Brian E. Mann,*[a] Philip Sawle,[b] Rehan Aqil,[c] Trevor Perrior[c] and Roberto Motterlini[b]

Received 30th March 2007, Accepted 21st May 2007
First published as an Advance Article on the web 19th September 2007
DOI: 10.1039/b704832g

A new group of CO-releasing molecules, CO-RMs, based on cyclopentadienyl iron carbonyls have been identified. X-Ray structures have been determined for $[(\eta\text{-}C_5H_4CO_2Me)Fe(CO)_2X]$, X = Cl, Br, I, NO_3, CO_2Me, $[(\eta\text{-}C_5H_4CO_2Me)Fe(CO)_2]_2$, $[(\eta\text{-}C_5H_4CO_2CH_2CH_2OH)Fe(CO)_2]_2$ and $[(\eta\text{-}C_5H_4CO_2Me)Fe(CO)_3][FeCl_4]$. Half-lives for CO release, ^1H, ^{13}C, and ^{17}OC NMR and IR spectra have been determined along with some biological data for these compounds, $[(\eta\text{-}C_5H_4CO_2CH_2CH_2OH)Fe(CO)_3]^+$ and $[\{\eta\text{-}C_5H_4(CH_2)_nCO_2Me\}Fe(CO)_3]^+$, n = 1, 2. More specifically, cytotoxicity assays and inhibition of nitrite formation in stimulated RAW264.7 macrophages are reported for most of the compounds analyzed. $[(\eta\text{-}C_5H_5)Fe(CO)_2X]$, X = Cl, Br, I, were also examined for comparison. Correlations between the half-lives for CO release and spectroscopic parameters are found within each group of compounds, but not between the groups.

Introduction

Carbon monoxide is a signalling molecule produced in mammals by the oxidation of heme by heme oxygenase. It is anti-inflammatory, protects against ischemia-reperfusion injury, prevents endothelial cell apoptosis, produces vasodilatation and protects against graft rejection. The biological role of CO is being investigated in animal models of disease for its possible use in a number of medical applications.[1] These include but are not restricted to organ transplantation,[2] cardiopulmonary bypass surgery,[3] and angioplasty.[4] More recently, administration of CO gas to animals has been shown to reverse established pulmonary hypertension.[5]

From the studies conducted so far, the general therapeutic approach is that CO would be provided as an additive to the air being breathed. However, due to the high toxicity of CO, great care is necessary to control the dose and protect the people administering and receiving the gas. Hence the use of solid CO-releasing molecules (CO-RMs) is highly attractive from a pharmaceutical point of view as the total quantity of CO being administered can be tightly controlled by weight and a solution of the molecules can be given where required to avoid the exposure of the whole body to CO.

Early attempts to devise CO-releasing molecules involved $[Fe(CO)_5]$, $[Mn(CO)_5]_2$ and $[Ru(CO)_3Cl_2]_2$.[6] $[Fe(CO)_5]$ and $[Mn(CO)_5]_2$ do not dissolve in water and photolysis was used to liberate the CO. These problems coupled with the high toxicity of $[Fe(CO)_5]$ resulted in a search for water-soluble CO-releasing molecules which were stable in solid form, but released CO when introduced into biological fluid at 37 °C. $[Ru(CO)_3Cl_2]_2$ partially met these problems. It had to be initially dissolved in DMSO in order to use it subsequently in aqueous solutions but in the process it lost a variable quantity of CO to give a mixture of $[Ru(CO)_3Cl_2(DMSO)]$ and $[Ru(CO)_2Cl_2(DMSO)_2]$ (isomers).[6]

$[Ru(CO)_3Cl_2]_2$ was modified to give $[Ru(CO)_3Cl(glycinate)]$ which is now well established as a CO-releasing molecule.[7] It has been used to provide CO for a wide range of biological applications such as protection of the heart against myocardial infarction[8] and the kidney against both ischaemia-induced acute renal failure,[9] and the toxic effects of cisplatin.[10]

More recently, $[H_3BCO_2]^{2-}$ (CORM-A1) has also been shown to provide CO which produces vasodilatation in isolated vessels and promotes a reduction in mean arterial pressure *in vivo*.[11]

In this report, the first viable CO-releasing molecules based on iron compounds are identified after an initial report in 2001.[12] A number of iron(0) compounds of the type [(η^4-substituted pyrone)$Fe(CO)_3$] have been reported in 2005 and 2006 as CO-releasing molecules. They release CO slowly and were published without patent protection.[13]

The known compound, $[(\eta\text{-}C_5H_5)Fe(CO)_3]Cl$, is water-soluble and slowly releases CO to myoglobin at 37 °C with a half-life of 69 min.[12] It produces vasodilatation when added to

[a]*Department of Chemistry, University of Sheffield, Sheffield, UK S3 7HF. E-mail: b.mann@sheffield.ac.uk; Fax: +44 (0)114 2738673; Tel: +44 (0)114 2229332*
[b]*Vascular Biology Unit, Department of Surgical Research, Northwick Park Institute for Medical Research, Harrow, Middlesex, UK E-mail: r.motterlini@imperial.ac.uk; Fax: +44 (0)208 8693538; Tel: +44 (0)208 8693181*
[c]*NCE Discovery Ltd., 418 Cambridge Science Park, Cambridge, UK CB4 0PZ. E-mail: t.perrior@ncediscovery.com; Fax: +44 (0)1223 433 181; Tel: +44 (0)1223 433 188*

† Based on the presentation given at Dalton Discussion No. 10, 3rd–5th September 2007, University of Durham, Durham, UK.

‡ CCDC reference numbers 640137–640144. For crystallographic data in CIF or other electronic format see DOI: 10.1039/b704832g

§ Electronic supplementary information (ESI) available: $[(\eta\text{-}C_5H_4CO_2CH_2CH_2OH)Fe(CO)_2]_2$ *cis–trans* ratio in solution, cytotoxicity of $[(\eta\text{-}C_5H_4CO_2)CH_3Fe(CO)_2Br]$ in murine RAW264.7 macrophages, X-ray crystal data. See DOI: 10.1039/b704832g

a rat aorta pre-contracted using phenylephrine. Unfortunately, after CO is released, the compound precipitates, probably due to the formation of a neutral compound which is insoluble in water. As these types of compounds are likely to be used therapeutically in the cardiovascular system, the precipitate could block micro-arteries leading to medical complications. In order to avoid this problem, substituents have been introduced into the cyclopentadienyl ring and the resulting compounds tested for CO release, water solubility and biological activity. In this paper, $[\{\eta\text{-}C_5H_4(CH_2)_nCO_2Me\}Fe(CO)_3]^+$, $n = 0$, 1, 2, along with $[(\eta\text{-}C_5H_4CO_2Me)Fe(CO)_2X]$, X = Cl, Br, I, NO_3, and $[\{\eta\text{-}C_5H_4CO_2(CH_2)_2OH\}Fe(CO)_3]^+$ are examined as CO-releasing molecules. Parameters such as $\delta(^{13}CO)$, $\delta(^{17}OC)$ and $\nu(CO)$ are examined as predictors of the rate of CO loss.

Results and discussion

At first sight, the synthesis of compounds of the type, $[(\eta\text{-}C_5H_4R)Fe(CO)_3]X$, should be easy. There are numerous examples of substituted ferrocenes,[14] but a literature search for examples of the cation $[(\eta\text{-}C_5H_4R)Fe(CO)_3]^+$ only yielded R = Me,[15] Et,[16] $CHPh_2$,[17] and OH.[18] However, there is much more literature regarding the synthesis of the dimeric compounds $[(\eta\text{-}C_5H_4R)Fe(CO)_2]_2$ containing functionality on the Cp ring.[19] In this work, the previously reported $[(\eta\text{-}C_5H_4CO_2Me)Fe(CO)_2]_2$[20] is used as a starting material to yield water-soluble CO-releasing molecules. $[(\eta\text{-}C_5H_4CO_2Me)Fe(CO)_2I]$ has been reported previously.[20]

The preparation of $[(\eta\text{-}C_5H_4CO_2Me)Fe(CO)_2]_2$ involves the synthesis of $C_5H_5CO_2Me$ from $[C_5H_5]^-$ and $ClCO_2Me$. $C_5H_5CO_2Me$ readily dimerises by the Diels–Alder reaction so it is reacted immediately with $[Fe_2(CO)_9]$ to give the product. The use of $[Fe_2(CO)_9]$ rather than the published route using $[Fe(CO)_5]$ is preferred as in our hands the synthesis proved to be more reliable. $[(\eta\text{-}C_5H_4CO_2Me)Fe(CO)_2]_2$ was used to synthesise $[(\eta\text{-}C_5H_4CO_2Me)Fe(CO)_2X]$, X = CO_2Me, Cl, Br, I and NO_3 and $[(\eta\text{-}C_5H_4CO_2Me)Fe(CO)_3]^+$. Transesterification was used to convert $[(\eta\text{-}C_5H_4CO_2Me)Fe(CO)_2]_2$ to $[(\eta\text{-}C_5H_4CO_2CH_2CH_2OH)\text{-}Fe(CO)_2]_2$ to enhance the water solubility. Two routes[21,22,23] were used to convert $[(\eta\text{-}C_5H_4R)Fe(CO)_2]_2$ to $[(\eta\text{-}C_5H_4R)Fe\text{-}(CO)_3]^+$: (i) protonation of $[(\eta\text{-}C_5H_4CO_2Me)Fe(CO)_2(CO_2Me)]$ and (ii) reaction of $[(\eta\text{-}C_5H_4R)Fe(CO)_2]_2$ with oxidising agents such as SO_2Cl_2 or $[(\eta\text{-}C_5H_5)_2Fe]^+$ in the presence of CO.

In order to compare the effect of the CO_2Me substituent with an alkyl one, $[\{\eta\text{-}C_5H_4(CH_2)_nCO_2Me\}Fe(CO)_3]^+$, $n = 1$, 2, were also synthesised.

X-Ray crystal structures

The X-ray crystal structures of many of the compounds were determined. The X-ray crystal structure of $[(\eta\text{-}C_5H_4CO_2Me)Fe(CO)_2]_2$, (Fig. 1) is similar to those determined previously for many related compounds. The cyclopentadienyls are *trans* across the plane of the $Fe_2(\mu\text{-}CO)_2$ moiety as is commonly found.[24,25] In contrast, the X-ray crystal structure of $[(\eta\text{-}C_5H_4CO_2CH_2CH_2OH)Fe(CO)_2]_2$ shows the cyclopentadienyls *cis* across the plane of the $Fe_2(\mu\text{-}CO)_2$ moiety (Fig. 2) which is less common excluding those where bonding between the two cyclopentadienyl rings forces a *cis*-geometry.[26] In three of the cases of *cis*-geometries, there are Lewis acids

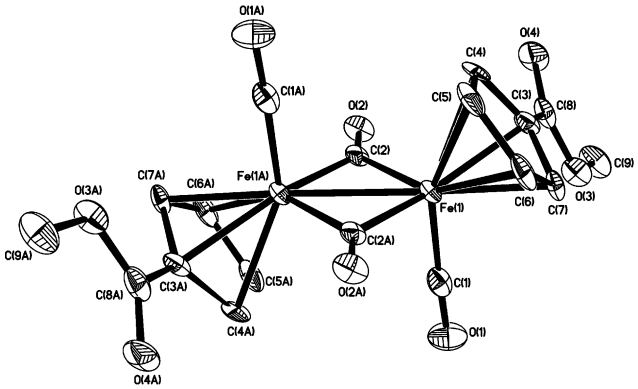

Fig. 1 The X-ray crystal structure of $[(\eta\text{-}C_5H_4CO_2Me)Fe(CO)_2]_2$. Selected bond lengths [Å]:- Fe1–Fe1 2.525(3), Fe1–C1 1.762(10), Fe1–C2 1.920(8), Fe1–C3 2.108(8), Fe1–C4 2.143(8), Fe1–C5 2.143(9), Fe1–C6 2.136(8), Fe1–C7 2.077(8). Thermal ellipsoids are shown at 50%.

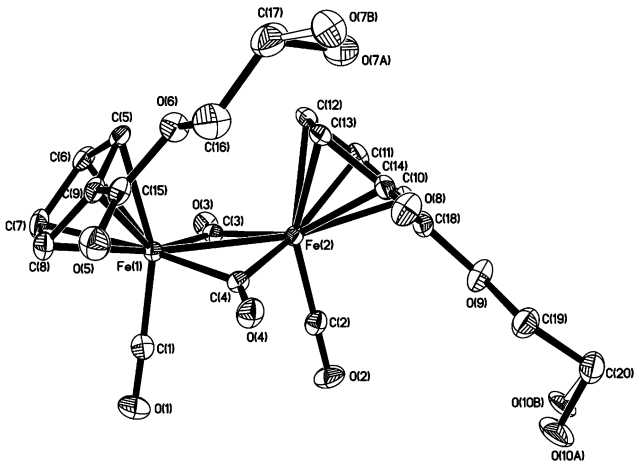

Fig. 2 The X-ray crystal structure of $[(\eta\text{-}C_5H_4CO_2CH_2CH_2OH)\text{-}Fe(CO)_2]_2$. O7 and O10 are disordered. Selected bond lengths [Å]:- Fe1–Fe2 2.5224(10), Fe1–C1 1.7633(19), Fe1–C3 1.920(2), Fe1–C4 1.9234(18), Fe1–C5 2.145(2), Fe1–C6 2.1434(18), Fe1–C7 2.0988(19), Fe1–C8 2.0915(19), Fe1–C9 2.1302(19), Fe2–C2 1.760(2), Fe2–C3 1.9336(18), Fe2–C4 1.914(2), Fe2–C10 2.0926(19), Fe2–C11 2.121(2), Fe2–C12 2.1293(19), Fe2–C13 2.1227(18), Fe2–C14 2.1135(19). Thermal ellipsoids are shown at 50%.

coordinated to the oxygen(s) of the bridging carbonyl(s). The *cis*-stereochemistry may be favoured by hydrogen bonding over a distance of 1.947 Å across the molecule between the $RCH_2O(7A)H$ substituent on one cyclopentadienyl and the O(8)=C(OMe)R on the other. This interaction is weak as O(7)H is disordered between two positions, one which hydrogen-bonds with a 51% occupancy and the atom in the other position does not. This hydrogen-bonding interaction is also small in solution as it makes no measurable contribution to the solution *cis–trans* ratio determined from IR spectra or the activation energy for carbonyl exchange of the bridge and terminal carbonyls in the *cis*-isomer *via* the *trans*-isomer. There is also disorder at the CH_2OH group.

The X-ray crystal structures of $[(\eta\text{-}C_5H_4CO_2Me)Fe(CO)_2Cl]$ (Fig. 3), $[(\eta\text{-}C_5H_4CO_2Me)Fe(CO)_2Br]$ (Fig. 4), $[(\eta\text{-}C_5H_4CO_2Me)\text{-}Fe(CO)_2I]$ (Fig. 5), $[(\eta\text{-}C_5H_4CO_2Me)Fe(CO)_2(NO_3)]$ (Fig. 6), $[(\eta\text{-}C_5H_4CO_2Me)Fe(CO)_2(CO_2Me)]$ (Fig. 7) and $[(\eta\text{-}C_5H_4CO_2\text{-}Me)Fe(CO)_3][FeCl_4]$ (Fig. 8) are very similar to those reported

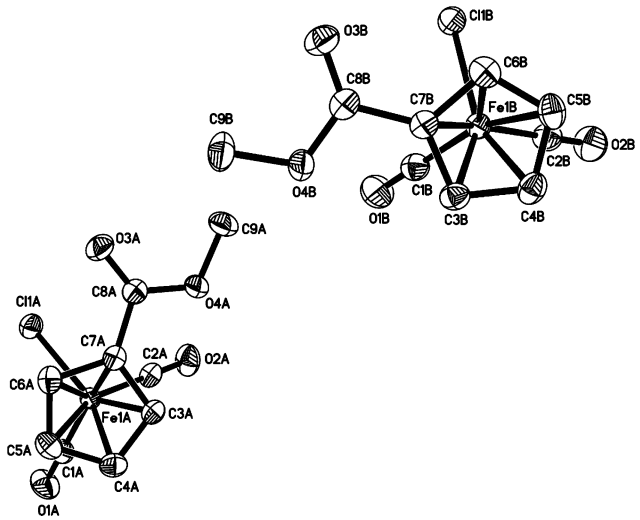

Fig. 3 The X-ray crystal structure of $[(\eta\text{-}C_5H_4CO_2Me)Fe(CO)_2Cl]$. Fe1A–C2A 1.788(2), Fe1A–C1A 1.792(2), Fe1A–C3A 2.081(2), Fe1A–C4A 2.090(2), Fe1A–C5A 2.125(2), Fe1A–C6A 2.1201(19), Fe1A–C7A 2.0829(19), Fe1A–Cl1A 2.2899(6), Fe1B–C1B 1.799(2), Fe1B–C2B 1.791(2), Fe1B–C3B 2.086(2), Fe1B–C4B 2.085(2), Fe1B–C5B 2.112(2), Fe1B–C6B 2.122(2), Fe1B–C7B 2.0919(18), Fe1B–Cl1B 2.2894(6). Thermal ellipsoids are shown at 50%.

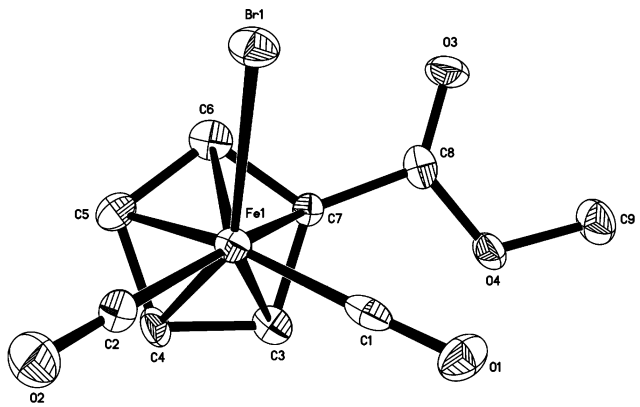

Fig. 4 The X-ray crystal structure of $[(\eta\text{-}C_5H_4CO_2Me)Fe(CO)_2Br]$. Selected bond lengths [Å]:- Fe1–C2 1.783(7), Fe1–C1 1.789(7), Fe1–C3 2.071(6), Fe1–C4 2.086(6), Fe1–C7 2.094(6), Fe1–C5 2.109(6), Fe1–C6 2.133(6), Fe1–Br1 2.4248(10). Thermal ellipsoids are shown at 50%.

previously for similar compounds. The structures of $[(\eta\text{-}C_5H_5)Fe(CO)_2Cl]$,[27] $[(\eta\text{-}C_5Me_5)Fe(CO)_2Cl]$,[28] $[(\eta\text{-}C_5Ph_5)Fe(CO)_2Br]$,[29] $[(\eta\text{-}C_5R_5)Fe(CO)_2I]$, R_5 = any substituent including H,[30,31,32,33] $[(\eta\text{-}C_5H_5)Fe(CO)_2(NO_3)]$,[34] and $[(\eta\text{-}C_5R_5)Fe(CO)_3]$, R_5 = any substituent including H,[23,33,35] have been reported previously. Some selected bond lengths are collected in Table 1.

There are some examples of X-ray crystal structures of the $[(\eta\text{-}C_5R_4CO_2Me)Fe(CO)_2X]$, R = any substituent including H, in the literature.[36,37,38] The closest literature examples are $[(\eta\text{-}C_5H_4CO_2H)Fe(CO)_2CH_3]$[38] and $[(\eta\text{-}C_5H_5)_2Ti\{(O_2CC_5H_4\text{-}\eta)Fe(CO)_2CH_2Ph\}_2]$.[37]

The introduction of the CO_2R substituent into the cyclopentadienyl ring appears to induce some bond localisation into the ring (Table 1). For most of the compounds individually, the differences in C–C bond lengths are not sufficiently different to prove the localisation when the standard deviation is taken into account. When all the compounds are taken together, the evidence for localisation is strong. The CO_2R group is nearly coplanar with the C_5H_4 ring with the O=C–C–C torsion angle, *A*, being close to 0° or 180°. The $(RO_2C)C$–(cyclopentadienyl ring centroid)–Fe–X torsion angle *B*, is near 60° in most cases, showing that the preferred conformation has the $(RO_2C)C$ group approximately bisecting the (OC)–Fe–X angle. In the case of $[(\eta\text{-}C_5H_4CO_2H)Fe(CO)_2Me]$ it approximately bisects the (OC)–Fe–(CO) angle. Only in the case of the dimer does it approximately eclipse an OC–Fe bond. For $[(\eta\text{-}C_5H_4CO_2Me)Fe(CO)_2(NO_3)]$, the nitrate O6 is only 2.854 Å from the carboxy carbon, C8. This causes the $(RO_2C)C$–(cyclopentadienyl ring centroid)–Fe–X torsion angle *B* to be close to 46°.

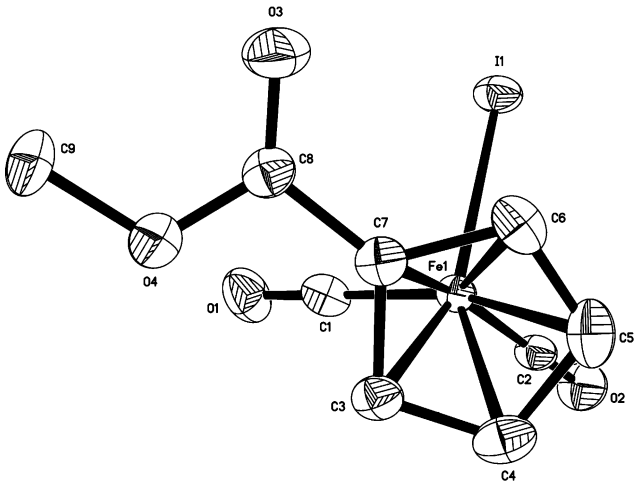

Fig. 5 The X-ray crystal structure of $[(\eta\text{-}C_5H_4CO_2Me)Fe(CO)_2I]$. Selected bond lengths [Å]:- Fe1–C1 1.776(5), Fe1–C2 1.793(5), Fe1–C3 2.086(4), Fe1–C4 2.098(4), Fe1–C5 2.116(4), Fe1–C6 2.130(4), Fe1–C7 2.106(4), Fe1–I1 2.6046(9). Thermal ellipsoids are shown at 50%.

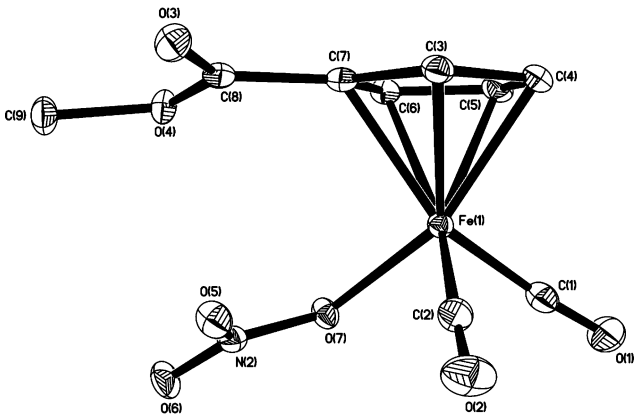

Fig. 6 The X-ray crystal structure of $[(\eta\text{-}C_5H_4CO_2Me)Fe(CO)_2(NO_3)]$. Selected bond lengths [Å]:- Fe1–C1 1.791(3), Fe1–C2 1.819(3), Fe1–C3 2.110(3), Fe1–C4 2.095(2), Fe1–C5 2.116(2), Fe1–C6 2.111(3), Fe1–C7 2.105(3), Fe1–O7 1.9729(17). Thermal ellipsoids are shown at 50%.

$[(\eta\text{-}C_5H_4CO_2R)Fe(CO)_2]_2$, R = Me, CH_2CH_2OH

It is well established that $[(\eta\text{-}C_5R_5)Fe(CO)_2]_2$, R_5 = any substituent including H, exists in solution as interconverting *cis*- and *trans*-isomers.[39,40,41] On account of the hydrogen bonding seen in the X-ray crystal structure of $[(\eta\text{-}C_5H_4CO_2CH_2CH_2OH)Fe(CO)_2]_2$,

Table 1 Selected bond lengths and angles for the $RO_2CC_5H_4$ group in $[(\eta\text{-}MeO_2CC_5H_4)Fe(CO)_2]_2$, $[(\eta\text{-}RO_2CC_5H_4)Fe(CO)_2X]$, and $[(\eta\text{-}MeO_2CC_5H_4)Fe(CO)_3][FeCl_4]$. *A* is the torsion angle between the O=C and C_5H_4 (C^7–C^6–C^1–C^2) ring and *B* is the torsion angle between C^1-centroid of C_5H_4 ring and the Fe–X bond taking X as $(\eta\text{-}MeO_2CC_5H_4)Fe(CO)_2$ in the case of the dimer. The atom numbering in Table 1 follows that in the diagram with the substituent of the iron being used to differentiate between C^2 and C^5 and C^3 and C^4

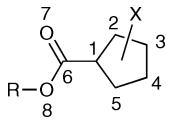

R	X	C^1–C^2/Å	C^2–C^3/Å	C^3–C^4/Å	C^4–C^5/Å	C^5–C^1/Å	C^1–C^6/Å	C^6–O^7/Å	*A*/°	*B*/°
Me	Dimer	1.417(13)	1.418(13)	1.418(14)	1.407(12)	1.439(11)	1.467(12)	1.214(11)	15.51	117.22
CH_2CH_2OH	Dimer	1.424(2)	1.416(3)	1.405(3)	1.420(3)	1.425(2)	1.473(2)	1.2058(17)	5.11	106.49
		1.428(3)	1.413(3)	1.411(3)	1.431(3)	1.411(3)	1.476(3)	1.203(2)	179.87	72.30
Me	Cl	1.423(3)	1.409(3)	1.435(3)	1.406(3)	1.436(3)	1.478(3)	1.206(2)	6.59	65.31
		1.432(3)	1.399(3)	1.439(3)	1.409(3)	1.440(3)	1.472(3)	1.209(2)	3.44	59.21
Me	Br	1.435(9)	1.410(9)	1.434(9)	1.391(8)	1.449(8)	1.477(8)	1.204(7)	4.41	70.21
Me	I	1.446(6)	1.385(7)	1.436(7)	1.411(7)	1.452(6)	1.464(6)	1.198(6)	4.41	68.83
Me	NO_3	1.426(3)	1.421(4)	1.434(4)	1.413(3)	1.429(4)	1.479(3)	1.206(3)	12.58	45.93
Me	CO_2Me	1.438(2)	1.402(2)	1.437(2)	1.412(2)	1.422(2)	1.482(2)	1.202(2)	1.80	68.76
Me	CO	1.4201(18)	1.4181(19)	1.432(2)	1.412(2)	1.4372(18)	1.4913(18)	1.2026(17)	10.09	—
H[38]	Me	1.425	1.404	1.419	1.406	1.429	1.462	1.2472(19)	2.12	178.36
Cp_2Ti[37,a]	CH_2Ph	1.433	1.387	1.420	1.379	1.412	1.484(8)	1.211(7)	5.67	64.59
		1.441	1.385	1.417	1.403	1.415	1.477(8)	1.206(7)	3.72	75.47

[a] $[Cp_2Ti\{(O_2CC_5H_4)Fe(CO)_2CH_2Ph\}_2]$.

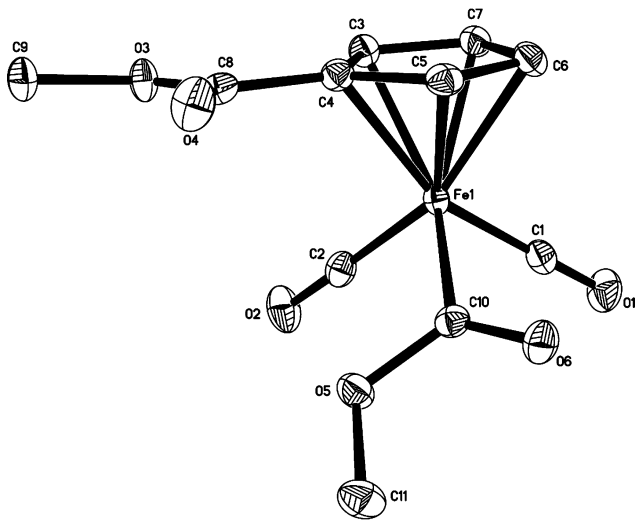

Fig. 7 The X-ray crystal structure of $[(\eta\text{-}C_5H_4CO_2Me)Fe(CO)_2(CO_2Me)]$. Selected bond lengths [Å]:- Fe1–C1 1.7689(19), Fe1–C2 1.7662(18), Fe1–C3 2.1028(19), Fe1–C4 2.0939(18), Fe1–C5 2.1150(17), Fe1–C6 2.1052(17), Fe1–C7 2.1111(18), Fe1–C10 1.9593(17). Thermal ellipsoids are shown at 50%.

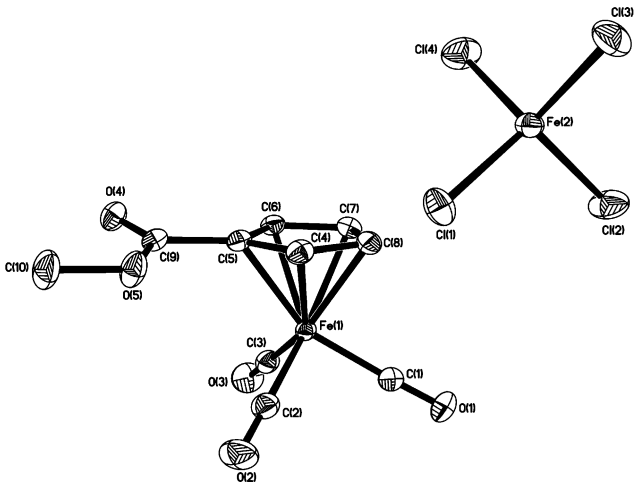

Fig. 8 The X-ray crystal structure of $[(\eta\text{-}C_5H_4CO_2Me)Fe(CO)_3][FeCl_4]$. Selected bond lengths [Å]:- Fe1–C1 1.8189(14), Fe1–C2 1.8242(15), Fe1–C3 1.8085(14), Fe1–C4 2.0991(13), Fe1–C5 2.0941(13), Fe1–C6 2.1099(13), Fe1–C7 2.0963(13), Fe1–C8 2.1042(13), Fe2–Cl1 2.1839(4), Fe2–Cl2 2.1928(4), Fe2–Cl3 2.1843(4), Fe2–Cl4 2.2026(4). Thermal ellipsoids are shown at 50%.

the ratio of *cis*- and *trans*-isomers has been determined using *ν*(CO) intensities to check if there is any preference for the *cis*-isomer[39] and by ^{13}C NMR measurements of $\Delta G^{\ddagger}$ for exchange between the bridging and terminal carbonyls.[41,42]

IR spectroscopy using *ν*(CO) intensities was used to determine the *cis*–*trans* ratio of the isomers of $[(\eta\text{-}C_5H_4CO_2R)Fe(CO)_2]_2$, R = Me, CH_2CH_2OH, as previously described.[39] The results are given in Table S1§. The results show that on going from R = Me to CH_2CH_2OH and in comparison with $[(\eta\text{-}C_5H_5)Fe(CO)_2]_2$, the presence of the CH_2CH_2OH group makes no significant difference in the ratio, showing that the hydrogen bond between the OH and C=O found in the crystal structure does not result in an enhanced concentration of the *cis*-isomer.

It has been previously observed that $[(\eta\text{-}C_5H_5)Fe(CO)_2]_2$ shows at low temperatures, (*e.g.* −60 °C) two ^{13}CO signals for the *cis*-isomer due to the bridging and terminal carbonyls and one averaged ^{13}CO signal for the *trans*-isomer. On warming, the signals broaden and average due to carbonyl bridge-opening coupled with Fe–Fe bond rotation.[41,42] $\Delta G^{\ddagger}$ was determined for bridge–terminal carbonyl exchange in CD_2Cl_2 for *cis*-$[(\eta\text{-}C_5H_4CO_2R)Fe(CO)_2]_2$, R = Me, CH_2CH_2OH, $\Delta G^{\ddagger}_{244} = 51 \pm 3$ kJ mol^{-1} for R = CH_3 and $\Delta G^{\ddagger}_{258} = 54 \pm 3$ kJ mol^{-1} for R = CH_2CH_2OH. These values of $\Delta G^{\ddagger}$ do not differ significantly from 51 ± 3 kJ mol^{-1}

previously reported for *cis*-[(η-C_5H_5)Fe(CO)$_2$]$_2$, once again confirming that any interaction between the OH and C=O in [(η-$C_5H_4CO_2CH_2CH_2OH$)Fe(CO)$_2$]$_2$ is negligible.[42]

CO loss in solution

As the [(η-$C_5H_4CO_2R$)Fe(CO)$_2$X]$^{0/+}$ compounds were made as CO-releasing molecules for possible pharmaceutical use, the CO release was measured by using electronic spectroscopy to monitor the formation of carboxymyoglobin from myoglobin at 37 °C. The technique works well for about the first 60 min but after this time, the results become suspect. The result is that half-lives for CO loss of up to about 200 min are reasonably accurate but longer times have less accuracy. The electronic spectra were measured between 500 and 600 nm and fitted as a weighted sum of the spectra of myoglobin and carboxymyoglobin. Allowance was made for turbidity by applying a λ^{-4} correction to the spectrum. The spectra were fitted in Excel using the Solver routine.

A typical set of electronic spectra for [(η-$C_5H_4CO_2Me$)-Fe(CO)$_2$Br] are shown in Fig. 9 and the corresponding plot of CO concentration against time with a first order rate fit is shown in Fig. 10.

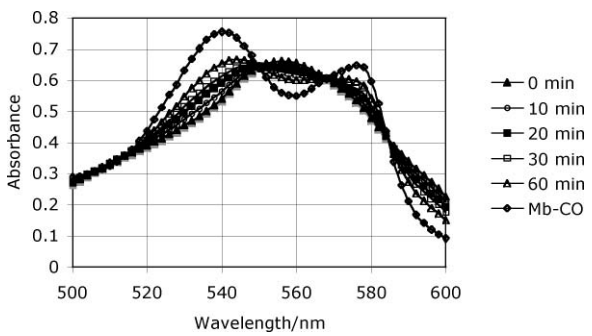

Fig. 9 The changes in the electronic spectrum of myoglobin as CO is released from [(η-$C_5H_4CO_2Me$)Fe(CO)$_2$Br] at 37 °C as a function of time. An extra spectrum is included. The curve marked Mb–CO is due to the myoglobin after saturation with CO gas. The spectra are shown after baseline correction.

The half-lives ($t_{1/2}$) for CO loss are collected in Table 2 along with ν(CO), δ(^{13}CO), δ(^{17}OC) and r(Fe–C). Within each group of compounds, [(η-C_5H_4R)Fe(CO)$_3$]$^+$ and [(η-$C_5H_4CO_2Me$)Fe(CO)$_2$X] there is an approximate correlation between $t_{1/2}$ and ν(CO), δ(^{13}CO), δ(^{17}OC) and r(Fe–C) but there is no correlation between

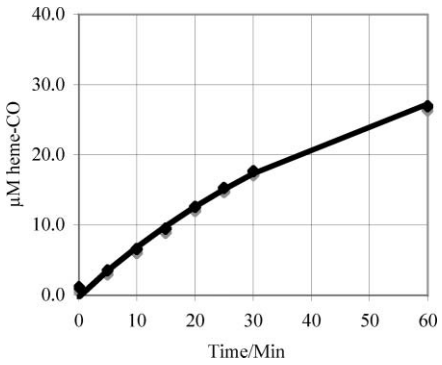

Fig. 10 A plot of CO released from 40 μM [(η-$C_5H_4CO_2Me$)Fe(CO)$_2$Br] to myoglobin at 37 °C as a function of time and the first order rate fit.

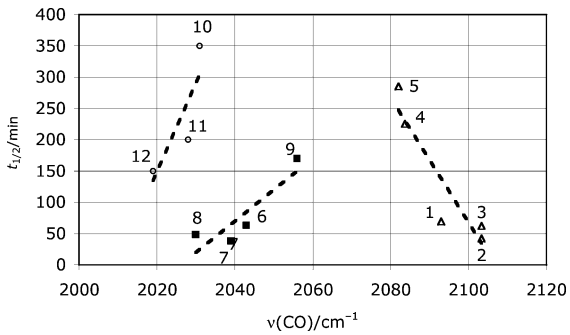

Fig. 11 A plot of half-lives for CO-loss against the average ν(CO) for ■, [(η-C_5H_4R)Fe(CO)$_3$]$^+$, R = H, **1**, CO_2Me, **2**, $CO_2CH_2CH_2OH$, **3**, CH_2CO_2Me, **4**, $(CH_2)_2CO_2Me$, **5**; △, [(η-$C_5H_4CO_2Me$)Fe(CO)$_2$X], X = Cl, **6**, Br, **7**, I, **8**, NO_3, **9**; ○, [(η-C_5H_5)Fe(CO)$_2$X], X = Cl, **10**, Br, **11**, I, **12**. Note that the average ν(CO) is calculated for [(η-C_5H_4R)Fe(CO)$_3$]$^+$ giving a double weighting to the lower frequency E symmetry band. Trend lines are included for the three groups of compounds.

the two sets of compounds. This is illustrated for ν(CO) in Fig. 11, δ(^{13}CO) in Fig. 12 and δ(^{17}OC) in Fig. 13. The correlation with r(Fe–C) is relatively poor probably due to the errors in determining both $t_{1/2}$ and r(Fe–C).

The graphs show some correlation between $t_{1/2}$ and ν(CO), δ(^{13}CO), δ(^{17}OC) within a group of compounds, but no correlation overall.

When the data for the series [(η-C_5H_5)Fe(CO)$_2$X] is compared with those from [(η-$C_5H_4CO_2Me$)Fe(CO)$_2$X], the introduction of the CO_2Me substituent results in ν(CO), r(CO) and δ(^{17}OC)

Table 2 The half-lives for CO loss, ν(CO), δ(^{17}O), δ(^{13}C), and r(Fe–CO)

Compound/Ion	$t_{1/2}$/min	ν(CO)/cm^{-1}	δ(^{17}O) (ppm)	δ(^{13}C) (ppm)	Average r(Fe–CO)/Å
[(C_5H_5)Fe(CO)$_3$]$^+$	69	2125, 2077	388.2	202.4	1.816
[($C_5H_4CO_2Me$)Fe(CO)$_3$]$^+$	42	2132, 2089	399.2	202.7	1.8172
[($C_5H_4CO_2CH_2CH_2OH$)Fe(CO)$_3$]$^+$	62	2132, 2089	391.2	200.6	—
[($C_5H_4CH_2CO_2Me$)Fe(CO)$_3$]$^+$	225	2121, 2065	—	204.7	—
[($C_5H_4CH_2CH_2CO_2Me$)Fe(CO)$_3$]$^+$	285	2116, 2065	—	203.7	—
[($C_5H_4CO_2Me$)Fe(CO)$_2$Cl]	63	2064, 2022	386.4	210.5	1.793
[($C_5H_4CO_2Me$)Fe(CO)$_2$Br]	38	2060, 2018	385.7	210.8	1.786
[($C_5H_4CO_2Me$)Fe(CO)$_2$I]	48	2050, 2010	384.9	212.0	1.785
[($C_5H_4CO_2Me$)Fe(CO)$_2$(NO_3)]	170	2076, 2036	393.7	209.0	1.805
[(C_5H_5)Fe(CO)$_2$Cl]	350	2054, 2008	383.1	212.4	1.771[27]
[(C_5H_5)Fe(CO)$_2$Br]	200	2051, 2005	382.3	212.5	—
[(C_5H_5)Fe(CO)$_2$I]	150	2041, 1997	381.2	213.5	1.781[31]

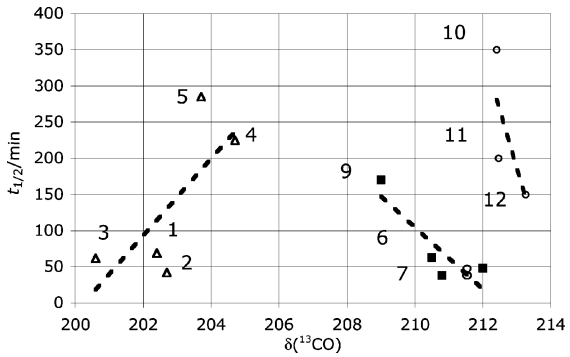

Fig. 12 A plot of half-lives for CO-loss against the $\delta(^{13}CO)$ for ■, $[(\eta\text{-}C_5H_4R)Fe(CO)_3]^+$, R = H, **1**, CO_2Me, **2**, $CO_2CH_2CH_2OH$, **3**, CH_2CO_2Me, **4**, $(CH_2)_2CO_2Me$, **5**; △, $[(\eta\text{-}C_5H_4CO_2Me)Fe(CO)_2X]$, X = Cl, **6**, Br, **7**, I, **8**, NO_3, **9**; ○, $[(\eta\text{-}C_5H_5)Fe(CO)_2X]$, X = Cl, **10**, Br, **11**, I, 12. Trend lines are included for the three groups of compounds.

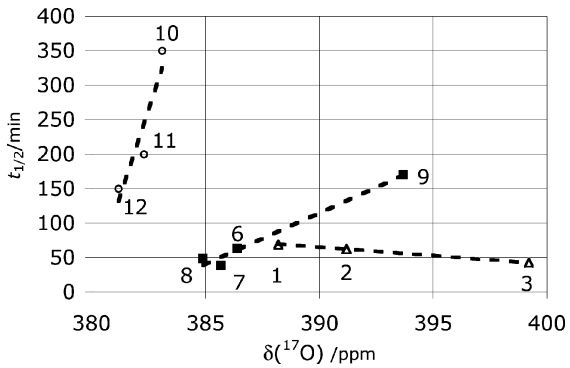

Fig. 13 A plot of half-lives for CO-loss against the $\delta(^{17}OC)$ for ■, $[(\eta\text{-}C_5H_4R)Fe(CO)_3]^+$, R = H, **1**, CO_2Me, **2**, $CO_2CH_2CH_2OH$, **3**, CH_2CO_2Me, **4**, $(CH_2)_2CO_2Me$, **5**; △, $[(\eta\text{-}C_5H_4CO_2Me)Fe(CO)_2X]$, X = Cl, **6**, Br, **7**, I, **8**, NO_3, **9**; ○, $[(\eta\text{-}C_5H_5)Fe(CO)_2X]$, X = Cl, **10**, Br, **11**, I, 12. Trend lines are included for the three groups of compounds.

increasing while $\delta(^{13}CO)$ decreases. This is consistent with the CO_2Me substituent withdrawing electron density from the metal weakening the M–CO bond.

For the cations, $[(\eta\text{-}C_5H_4R)Fe(CO)_3]^+$, $t_{1/2}$ decreases as ν(CO) increases towards the value of free CO. The data are consistent with a weakening in the Fe–CO bond paralleling the ease of loss of CO as might be expected for a dissociative reaction. The reverse is found for $[(\eta\text{-}C_5H_5)Fe(CO)_2X]$ and $[(\eta\text{-}C_5H_4CO_2Me)Fe(CO)_2X]$. As ν(CO) increases and the Fe–CO bond lengthens, $t_{1/2}$ gets longer.

These results show that within a series of compounds, ν(CO), $\delta(^{13}CO)$ and $\delta(^{17}OC)$ could be of value in predicting which compounds may release CO rapidly. The prediction is not easy as the effect of substituents may differently affect the ground and transition states. Caution is necessary as the number of compounds is limited.

Biological activity

The compounds were tested for biological activity using murine RAW264.7 macrophages exposed to three different concentrations of the CO-RM (10, 50 and 100 μM). After 24 h treatment, three tests were performed on the macrophages.

Alamar blue was used to test the redox activity of the cells. The results for $[(\eta\text{-}C_5H_4CO_2Me)Fe(CO)_2Br]$ are shown in Fig. 14,

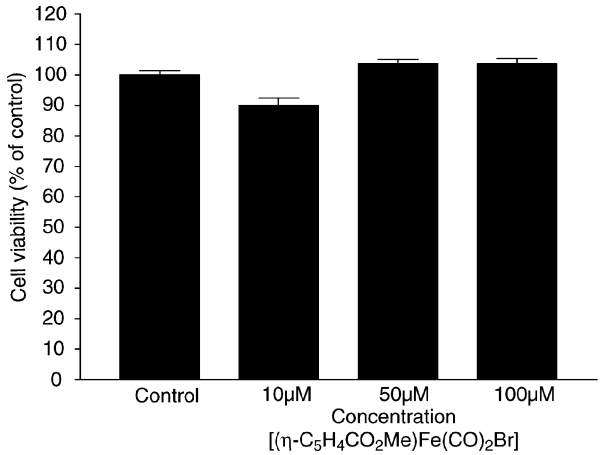

Fig. 14 Cell viability in murine RAW264.7 macrophages exposed for 24 h to 10, 50 and 100 μM $[(\eta\text{-}C_5H_4CO_2Me)Fe(CO)_2Br]$. The percentage of viable cells was assessed using an Alamar Blue assay.

where it can be seen that even at 100 μM there is no reduction in activity.

The release of lactic dehydrogenase (LDH) in the medium of the cells was used as a test for cytotoxicity. A reference for 100% cytotoxicity was generated by adding Triton to the cells. The results for $[(\eta\text{-}C_5H_4CO_2Me)Fe(CO)_2Br]$ are shown in Fig. S1§, where it can be seen that even at 100 μM there is no detectable toxicity.

One of the key roles of CO *in vivo* is its ability to reduce inflammation caused by over-production of NO in macrophages. The production of NO can be estimated by determining nitrite formation and this is shown in Fig. 15. Lipopolysaccharide (LPS) is used to stimulate NO production from macrophages and the effectiveness of the CO-RM in reducing NO and hence nitrite formation is determined. Examination of Fig. 15 shows that addition of $[(\eta\text{-}C_5H_4CO_2Me)Fe(CO)_2Br]$ to produce a 10 μM solution has no effect while both the 50 and 100 μM solutions have a slight effect in inducing nitrite production. After the addition of LPS to induce nitrite formation, a 10 μM solution has no effect while both the 50 and 100 μM solutions have a major significant effect in reducing the amount of nitrite formed.

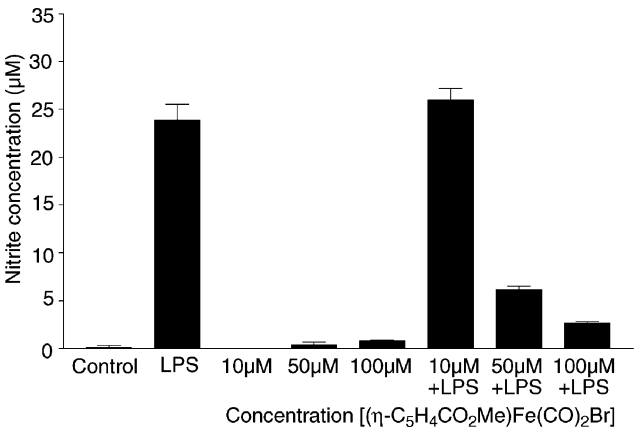

Fig. 15 Nitrite levels, an index of NO formation, in the media of murine RAW264.7 macrophages exposed for 24 h to 10, 50 and 100 μM $[(\eta\text{-}C_5H_4CO_2Me)Fe(CO)_2Br]$. 1 μg mL^{-1} LPS was used to induce nitrite formation and to test the effectiveness of $[(\eta\text{-}C_5H_4CO_2Me)Fe(CO)_2Br]$ in suppressing nitrite formation.

Table 3 Tests of biological activity of $[\{\eta\text{-}C_5H_4(CH_2)_nCO_2Me\}Fe(CO)_3]^+$, n = 0–2, $[(\eta\text{-}C_5H_4CO_2CH_2CH_2OH)Fe(CO)_3]^+$, $[(\eta\text{-}C_5H_4CO_2Me)Fe(CO)_2X]$, X = Cl, Br, I, NO_3 and $[(\eta\text{-}C_5H_5)Fe(CO)_2X]$, X = Cl, Br, I on the cell viability, cell toxicity and $[NO_2]^-$ formation by murine RAW264.7 monocyte macrophages. The * convention is explained below and is based on more * indicate the better the outcome. NA is not available

Compound/ion	Cell viability	Cytotoxicity	$[NO_2]^-$
$[(C_5H_4CO_2Me)Fe(CO)_3]^+$	***	***	*
$[(C_5H_4CO_2CH_2CH_2OH)Fe(CO)_3]^+$	***	***	*
$[(C_5H_4CH_2CO_2Me)Fe(CO)_3]^+$	***	***	*
$[(C_5H_4CH_2CH_2CO_2Me)Fe(CO)_3]^+$	***	***	*
$[(C_5H_4CO_2Me)Fe(CO)_2Cl]$	***	***	**
$[(C_5H_4CO_2Me)Fe(CO)_2Br]$	***	***	**
$[(C_5H_4CO_2Me)Fe(CO)_2I]$	***	***	**
$[(C_5H_4CO_2Me)Fe(CO)_2(NO_3)]$	***	***	**
$[(C_5H_5)Fe(CO)_2Cl]$	***	NA	NA
$[(C_5H_5)Fe(CO)_2Br]$	***	***	*
$[(C_5H_5)Fe(CO)_2I]$	***	***	*

* Greater than 50% cell viability or less than 50% cell toxicity at 10 μM CO-RM concentration or greater than 50% nitrite production inhibition at 100 μM CO-RM concentration.** Greater than 50% cell viability or nitrite production inhibition, or less than 50% cell toxicity at 50 μM CO-RM concentration.*** Greater than 50% cell viability or less than 50% cell toxicity at 100 μM CO-RM concentration or greater than 50% nitrite production inhibition at 10 μM CO-RM concentration.

The biological test results are reported in Table 3. All the compounds tested show excellent cell viability and cytotoxicity profiles. The compounds also reduce nitrite formation with the neutral compounds having limited ability while the cations tested have good ability. The presence of the ester group on the cyclopentadienyl ring provides a site to add different side chains to control water/lipid solubility and to include groups to direct the compounds to specific sites in the body.

Conclusions

The introduction of a substituent into the cyclopentadienyl ring of $[(C_5H_4CO_2R)Fe(CO)_3]^+$ and $[(C_5H_4CO_2R)Fe(CO)_2X]$ can be used to control the rate of CO release. For example, the introduction of a CO_2R group into the cyclopentadienyl group of $[(\eta\text{-}C_5H_4CO_2R)Fe(CO)_2X]$ increases the rate of CO loss to myoglobin. At the three concentrations tested (10, 50 and 100 μM), no significant reduction in cell viability or toxicity was found for any of the compounds tested. All the compounds show some activity in inhibiting nitrite formation by LPS-stimulated macrophages. Further biological testing is required to assess their usefulness in a wider range of biological applications. Within a small group of compounds, $\delta(^{13}CO)$, $\delta(^{17}OC)$ and $\nu(CO)$ correlate with the rate of CO loss but there is little correlation between the groups of compounds.

Experimental

Starting materials and reagents were purchased from Aldrich or Acros. $[Fe_2(CO)_9]$[43] and $[(C_5H_5)Fe(CO)_2X]$,[44] X = Cl, Br, I, were synthesised according to the literature. Solvents were dried using a Grubbs system (column chromatography), including DCM, THF, toluene, diethyl ether, hexane and petroleum ether. NMR experiments were carried out on a Bruker AVANCE 500, a Bruker AMX400 NMR spectrometer or a Bruker AC 250 NMR spectrometer. The temperature of the sample was measured by replacing it with another NMR tube containing the same solvent and a thermocouple attached to a Comark Evolution N9009 thermometer. Elemental analysis was carried out on a Perkin Elmer 2400 CHNS/O Series II Elemental analyser. IR spectra were recorded on a Bruker TENSOR 27 FT-IR spectrometer or a Perkin Elmer PARAGON 1000 FT-IR spectrometer. Mass spectrometry was carried out on either a Waters LCT Electrospray TOF Mass spectrometer ($ES^{\pm}$) or a VG Autospec Magnetic Sector Mass spectrometer (EI and FAB). X-Ray data collected were measured on a Bruker Smart CCD area detector with Oxford Cryosystems low temperature system. The release of CO from metal carbonyl complexes was determined spectrophotometrically by measuring the conversion of deoxymyoglobin (deoxy-Mb) to carbonmonoxy myoglobin (MbCO) as previously described.[6] The electronic spectra were measured between 500 and 600 nm at time intervals of 0, 5, 10, 15, 20, 25, 30 and 60 min and fitted as a weighted sum of the spectra of myoglobin and carboxymyoglobin. Allowance was made for any turbidity by applying a λ^{-4} correction to the spectrum. The spectra were fitted using Excel and Solver. The resulting concentrations were then fitted as first-order kinetics.

$C_5H_4CO_2Me$[20,45]

A solution of LiCp was prepared by the addition of 156.3 mL (0.25 mol) of n-BuLi (1.6 M in hexanes) to 20.65 mL (0.25 mol) of freshly cracked cyclopentadiene in 280 mL of dry THF at −78 °C, under argon. After complete addition, the reaction was allowed to warm slowly to room temperature and then stirred for a further hour. During this time a white precipitate is formed. Following this, the reaction was recooled to −78 °C and 19.3 mL (0.25 mol) of methyl chloroformate added dropwise. This resulted in complete disappearance of the white precipitate and the formation of a yellow–orange coloured solution. After warming to room temperature and then stirring for a further hour, a white precipitate was produced (LiCl). 500 mL of water was added and the two layers separated. The aqueous layer was washed with two 100 mL portions of diethyl ether, and then the combined organic extracts were washed with five 250 mL portions of water then once with saturated brine. It was then dried ($MgSO_4$ at 0 °C for 45 min) and then the solvent removed on a rotary evaporator to give a yellow oil. This was used without further purification.

$[(\eta\text{-}C_5H_4CO_2Me)Fe(CO)_2]_2$

All of the substituted cyclopentadiene synthesised in the above reaction was refluxed with 20 g of $[Fe_2(CO)_9]$ in 200 mL of deoxygenated heptane (argon purge), under argon for 24 h. Following this it was cooled to −18 °C overnight and then the purple crystalline precipitate collected on a sinter and washed with several portions of pentane. The heptane supernatant was recycled in repeats of the preparation and in this way yields can vary from 4.5 to 6 g (9.57 to 12.8). M_r = 469.99. ^1H NMR (400 MHz, CD_2Cl_2): δ 3.96 (s, Me, 3H), 5.03 (br, Cp, 2H), 5.29 (br, Cp, 2H). ^{13}C NMR (100.6 MHz, CD_2Cl_2, −29 °C): δ 52.6 (Me), 88.4 (Cp), 91.1 (Cp), 92.6 (*ipso* Cp), 164.7 (C=O), 208.7 (CO), 265.9 (CO). IR (CH_2Cl_2) $\nu(cm^{-1})$: 2010 (s), 1972 (m), 1724 (m). Mass spec. (m/z): 470 (M^+). Elemental: $Fe_2C_{18}H_{14}O_8$ found (calc) C: 45.60 (46.00), H: 2.79 (3.00).

[(η-$C_5H_4CO_2Me$)Fe$(CO)_2(CO_2Me)$]

A solution of [Fe$(CpCO_2Me)(CO)_2]_2$ (2 g, 4.26 mmol) in THF (30 mL) was added to a sodium amalgam (10 cm^3 mercury; 0.8 g (34.8 mmol) sodium). The mixture was stirred vigorously for 1 h. The resulting brown solution of Na[(η-$C_5H_4CO_2Me$)Fe$(CO)_2$] was transferred *via* syringe into a second flask. The solution was cooled to −78 °C and methyl chloroformate (0.657 mL) was added dropwise. The reaction mixture was stirred at room temperature for 3 h, during which time the reaction was monitored by IR spectroscopy. Removal of the solvent gave an oily residue which was redissolved in DCM, filtered and washed through Celite. The solvent was removed from the filtrate and an oily red residue was obtained. The product was dissolved in the minimum amount of hexane and left to recrystallise at −78 °C. A brown–yellow solid was obtained. Further crystallisation was carried out using DCM–hexane mixture which yielded a yellow crystalline solid. 802 mg (2.73 mmol) of product was obtained. M_r = 294.04. Yield 32%. ^{1}H NMR (400 MHz, d_6-acetone): δ 5.75 (s, 2H, Cp), 5.25 (s, 2H, Cp), 3.8 (s, 3H, Me), 3.5 (s, 3H, Me). ^{13}C NMR (100.62 MHz, d_6-acetone): δ 51.5 (CH_3), 51.7 (CH_3), 86.4 (*ipso* Cp), 87.4 (β-Cp), 90.7 (α-Cp), 164.6 (Cp C=O), 195.7 (Fe C=O), 212.7 (CO). IR (CH_2Cl_2) ν(cm^{-1}): 2044 (s), 1993 (s), 1727 (m). Mass spec. (*m*/*z*): 317 (M + Na^+). Elemental: $FeC_{11}H_{10}O_6$ found (calc) C: 45.01 (44.93), H: 3.33 (3.43).

[(η-$C_5H_4CO_2Me$)Fe$(CO)_3$][$FeCl_4$]

400 mg (0.851 mmol) of [(η-$C_5H_4CO_2Me$)Fe$(CO)_2]_2$ was dissolved in 20 mL of benzene, under argon. A solution of SO_2Cl_2 in benzene was then added dropwise with stirring. This resulted in the immediate formation of a yellow precipitate. The reaction was followed by IR spectroscopy, and when there was no more of the dimer starting material present, addition was ceased. The resulting precipitate was collected on a sinter and then washed with benzene and a little cold DCM. It was then recrystallised from DCM (*i.e.* sample dissolved in boiling DCM and then cooled to −18 °C overnight). The resulting yellow crystals were isolated, washed with diethyl ether and then dried under vacuum. 101 mg (0.219 mmol) of product obtained. M_r = 460.66. Yield 26%. X-Ray quality crystals were obtained from a dilute solution in MeCN–diethyl ether–pentane at −18 °C. ^{1}H NMR (400 MHz, CD_3CN): v. broad due to paramagnetic counter ion. ^{13}C NMR (100.62 MHz, CD_3CN): δ 60.6 (CH_3), 91.3 (*ipso* Cp), 97.2 (Cp), 99.8 (Cp), 161.7 (C=O), 202.7 (CO). ^{17}O NMR (54.2 MHz, CD_3CN): δ 399.2 (CO). IR (MeCN) ν(cm^{-1}): 2132 (s), 2089 (vs), 1745 (m). Mass spec. (*m*/*z*): 263 (M^+), 235 (M^+ − CO), 207 (M^+ − 2CO). Elemental: $Fe_2C_{10}H_7O_5Cl_4$ found (calc) C: 26.14 (26.07), H: 1.62 (1.53), Cl: 30.80 (30.78).

[(η-$C_5H_4CO_2Me$)Fe$(CO)_3$][BF_4]

Two drops of acid (HBF_4) were added to a vigorously stirred solution of [(η-$C_5H_4CO_2Me$)Fe$(CO)_2CO_2Me$] (80 mg, 0.272 mmol) in THF (10 mL). A white–yellow precipitate was formed instantaneously, this solid was filtered off using a sinter and washed twice with anhydrous diethyl ether. 77 mg (0.221 mmol) of product was obtained. M_r = 349.81. Yield 81%. ^{1}H NMR (400 MHz, CD_3OD): δ 6.55 (s, 2H, Cp), 6.0 (s, 2H, Cp), 3.9 (s, 3H, OMe). IR (CH_2Cl_2) ν(cm^{-1}): 2132(s), 2088(s), 1744(m). Elemental: $FeC_{10}H_7O_5BF_4$ found (calc) C: 34.12 (34.34), H: 1.93 (2.02).

[(η-$C_5H_4CO_2Me$)Fe$(CO)_2$Cl]

500 mg (1.06 mmol) of [(η-$C_5H_4CO_2Me$)Fe$(CO)_2]_2$ was dissolved in 14 mL of dry THF, under argon. A solution of 127 mg (1.06 mmol) of $SOCl_2$ in 5 mL dry THF was then added drop-wise with stirring. After complete addition, stirring was continued for a further 25 min. Following this, IR showed that there was still some starting material present. Hence a dilute THF solution of $SOCl_2$ was prepared and aliquots of this were added. The reaction was stirred until complete being monitored by IR spectroscopy. The solvent was removed on a rotary evaporator and the residue columned on silica gel, initially prepared in petroleum ether and eluted as a red band with diethyl ether. The solvent was removed on a rotary evaporator and the product recrystallised from diethyl ether–petroleum ether. 252 mg (0.932 mmol) of a red crystalline solid was obtained. M_r = 270.45. Yield 44%. X-Ray quality crystals were grown from diethyl ether at −18 °C. ^{1}H NMR (400 MHz, CD_2Cl_2): δ 3.93 (s, Me, 3H), 5.18 (br, Cp, 2H), 5.70 (br, Cp, 2H). ^{13}C NMR (100.62, CD_2Cl_2): δ 52.7 (Me), 83.0 (Cp), 84.5 (Cp *ipso*), 91.6 (Cp), 164.4 (C=O), 210.5 (CO). ^{17}O NMR (54.2 MHz, CD_2Cl_2): δ 386.4 (CO). IR (CH_2Cl_2) ν(cm^{-1}): 2064 (s), 2022 (s). Mass spec. (*m*/*z*): 270 (M^+), 242 (M^+ − CO), 214 (M^+ − 2CO). Elemental: $FeC_9H_7O_4Cl$ found (calc) C: 39.77 (39.97), H: 2.34 (2.61), Cl: 12.94 (13.11).

[(η-$C_5H_4CO_2Me$)Fe$(CO)_2$Br]

400 mg (0.851 mmol) of [(η-$C_5H_4CO_2Me$)Fe$(CO)_2]_2$ was dissolved in 20 mL of DCM, under argon. A solution of 150 mg (0.936 mmol) of Br_2 in 5 mL of DCM was then added drop-wise with stirring. After complete addition, stirring was continued for a further 30 min, after which time the reaction was shown to be complete by IR spectroscopy. The reaction solution was then transferred to a separating funnel and more DCM was added. It was washed with three portions of deoxygenated $Na_2S_2O_3$ (aq.) and once with deoxygenated water. Then it was dried ($MgSO_4$), filtered, and the solvent removed on a rotary evaporator to give a red–brown solid. A silica gel column was prepared in petroleum ether (40–60 °C). The product was introduced as a solution in a little DCM and eluted with petroleum ether containing increasing amounts of diethyl ether to (2 : 3) as a dark red band. Removal of solvent gave the product as a dark red solid, which was dried *in vacuo*. 268 mg (0.851 mmol) of product obtained. M_r = 314.90. Yield 50%. X-Ray quality crystals were grown from a diethyl ether solution at −18 °C. ^{1}H NMR (400 MHz, CD_2Cl_2): δ 3.90 (s, Me, 3H), 5.19 (br, Cp, 2H), 5.70 (br, Cp, 2H). ^{13}C NMR (100.62 MHz, CD_2Cl_2): δ 52.7 (Me), 83.2 (Cp), 84.0 (Cp *ipso*), 90.8 (Cp), 164.3 (C=O), 210.8 (CO). ^{17}O NMR (54.2 MHz, CD_2Cl_2): δ 385.7 (CO). IR (CH_2Cl_2) ν(cm^{-1}): 2060 (s), 2018 (s). Mass spec. (*m*/*z*): 314 (M^+), 286 (M^+ − CO), 258 (M^+ − 2CO). Elemental: $FeC_9H_7O_4Br$ found (calc) C: 34.68 (34.33), H: 2.14 (2.24), Br: 25.16 (25.37).

[(η-$C_5H_4CO_2Me$)Fe$(CO)_2$I][20]

800 mg (1.70 mmol) of [(η-$C_5H_4CO_2Me$)Fe$(CO)_2]_2$ was dissolved in 40 mL of DCM, under argon. A solution of 497 mg (1.96 mmol) of I_2 in 20 mL of DCM was then added drop-wise with stirring. After

complete addition, stirring was continued for a further 3 h, after which time reaction was shown to be complete by IR spectroscopy. The reaction solution was then transferred to a separating funnel and more DCM was added. It was washed with three portions of deoxygenated $Na_2S_2O_3$ (aq.) and once with deoxygenated water. It was then dried ($MgSO_4$), filtered, and the solvent removed on a rotary evaporator to give a black solid. This was dried under vacuum. 1.03 g of product obtained. $M_r = 361.90$. Yield 84%. X-Ray quality crystals were obtained from a diethyl ether solution at −18 °C. ^{1}H NMR (400 MHz, CD_2Cl_2): δ 3.90 (s, Me, 3H), 5.13 (br, Cp, 2H), 5.72 (br, Cp, 2H). ^{13}C NMR (100.62 MHz, CD_2Cl_2): δ 52.6 (Me), 83.7 (Cp), 89.9 (Cp), 164.2 (C=O), 212.0 (CO). ^{17}O NMR (54.2 MHz, CD_2Cl_2): δ 384.9 (CO). IR (CH_2Cl_2) ν(cm^{-1}): 2050 (s), 2010 (s). Mass spec. (m/z): 362 (M^+), 334 ($M^+ - CO$), 306 ($M^+ - 2CO$). Elemental: $FeC_9H_7O_4I$ found (calc) C: 29.86 (29.87), H: 1.71 (1.95), I: 35.06 (35.07).

[(η-$C_5H_4CO_2Me$)Fe(CO)$_2$(NO_3)]

300 mg (0.638 mmol) of [(η-$C_5H_4CO_2Me$)Fe(CO)$_2$]$_2$ and 228 mg (1.34 mmol) of $AgNO_3$ were stirred together in 15 mL of acetone at 30 °C, under argon. The reaction was monitored by IR spectroscopy and after 1.5 h the reaction was shown to be complete. The solution was filtered through Celite and then the solvent removed on a rotary evaporator to give a red oily residue. Recrystallisation was attempted from DCM–hexane but this did not work. The compound was introduced in DCM to a silica gel column, prepared in petroleum ether (40–60 °C). Elution with petroleum ether–diethyl ether (1 : 1) gave a very small amount of a yellow band. The product was eluted as a bright red band with diethyl ether. Removal of solvent on a rotary evaporator, washing with petroleum ether and drying *in vacuo* gave the desired solid product. 78 mg of a bright red solid was obtained (0.263 mmol). $M_r = 297.00$. Yield 21%. X-Ray quality crystals were obtained from a diethyl ether solution at −18 °C. ^{1}H NMR (400 MHz, CD_2Cl_2): δ 3.93 (s, CH_3), 5.21 (br, Cp, 2H), 5.78 (br, Cp, 2H). ^{13}C NMR (100.62 MHz, CD_2Cl_2): δ 53.0 (Me), 82.7 (Cp), 83.9 (Cp *ipso*), 91.5 (Cp), 164.0 (C=O), 209.0 (CO). ^{17}O NMR (54.2 MHz, CD_2Cl_2): δ 393.7 (CO). IR (CH_2Cl_2) ν(cm^{-1}): 2076 (s), 2036 (s). Elemental: $FeC_9H_7NO_7$ found (calc) C: 35.73 (36.40), H: 2.44 (2.38), N: 4.66 (4.72).

[(η-$C_5H_4CO_2CH_2CH_2OH$)Fe(CO)$_2$]$_2$

1.01 g (2.16 mmol) of [(η-$C_5H_4CO_2Me$)Fe(CO)$_2$]$_2$ and 15 mg (0.375 mmol) of NaH (60% disp. in mineral oil) were stirred in 18 mL of ethylene glycol at 55 °C overnight, under argon. DCM and deoxygenated water were added and the two layers separated. The aqueous layer was washed with DCM and then the combined DCM extracts were washed three times with deoxygenated water and once with saturated brine. It was then dried ($MgSO_4$) and the solvent removed on a rotary evaporator. The resulting solid was washed with several portions of diethyl ether. 1.00 g (1.89 mmol) of a dark purple solid was obtained. $M_r = 530.04$. Yield 88%. The sample can be recrystallised from DCM–hexane but the yield is lowered to 62%. ^{1}H NMR (400 MHz, CD_2Cl_2): δ 3.02 (s, OH, 1H), 4.00 (br, CH_2, 2H), 4.50 (br, CH_2, 2H), 5.06 (br, Cp, 2H), 5.39 (br, Cp, 2H). ^{13}C NMR (100.62 MHz, CD_2Cl_2, −17 °C): δ 60.9 (CH_2), 67.2 (CH_2), 88.4 (Cp), 91.1 (Cp), 91.6 (Cp *ipso*), 164.3 (C=O), 208.1 (CO), 267.7 (CO). IR (CH_2Cl_2) ν(cm^{-1}): 2012 (s), 1975 (m), 1785 (s), 1721 (m). Mass spec. (m/z): 531 (MH^+). Elemental: $Fe_2C_{20}H_{18}O_{10}$ found (calc) C: 44.83 (45.32), H: 3.37 (3.42).

[(η-$C_5H_4CO_2CH_2CH_2OH$)Fe(CO)$_3$][PF_6]

500 mg (0.943 mmol) of [(η-$C_5H_4CO_2CH_2CH_2OH$)Fe(CO)$_2$]$_2$ and 615 mg (1.86 mmol, 0.985 eq.) of ferrocenium hexafluorophosphate were placed in a Schlenk tube under a CO atmosphere. 70 mL of a CO-saturated DCM–THF mixture (2 : 1) was then added and the reaction stirred for 2.5–3 d in the dark with periodic bubbling of CO through the solution. A yellow precipitate started to form and precipitation was completed by addition of diethyl ether (150 mL). After stirring for 10 min the product was collected on a sinter, and washed several times with diethyl ether. It was then extracted through the sinter with acetone and the solvent removed from the filtrate. Washing the residue with diethyl ether gave a dark yellow solid product which was dried *in vacuo*. 485 mg (1.11 mmol) of product was obtained. $M_r = 437.99$. Yield 60%. ^{1}H NMR (400 MHz, CD_3CN): δ 3.85 (br, CH_2), 4.38 (br, CH_2), 5.84 (br, Cp, 2H), 6.41 (br, Cp, 2H). ^{13}C NMR (100.6 MHz, CD_3CN): δ 59.4 (CH_2), 68.4 (CH_2), 84.0 (*ipso* Cp), 89.7 (Cp), 93.6 (Cp), 161.2 (C=O), 200.6 (CO). ^{17}O NMR (54.2 MHz, CD_3CN): δ 391.2 (CO). IR (CH_3CN) ν(cm^{-1}): 2132 (s), 2089 (vs), 1743 (m). Mass spec. (m/z): 293 (M^+), 209 ($M^+ - 3CO$). Elemental: $FeC_{11}H_9O_6PF_6$ found (calc) C: 30.53 (30.16), H: 1.91 (2.07).

Methyl iodoacetate

The following procedure is based on a modified literature method.[46] A mixture of methyl bromoacetate (20.00 g, 12.4 mL, 131 mmol) and sodium iodide (25.10 g, 167 mmol, 1.28 eq.) in acetone (90 mL) was stirred at room temperature for 15 h and then heated at 50 °C for 2 h. The reaction mixture was then cooled to ambient temperature, filtered to remove sodium bromide and the solid was washed with diethyl ether (2 x 50 mL). The filtrate was concentrated *in vacuo*, diluted with diethyl ether (100 mL) and the organic layer was washed with water (2 x 50 mL), brine (50 mL), dried (anhydrous sodium sulfate) and evaporated to give methyl iodoacetate (18.69 g, 93.46 mmol, 72%) as a dark red oil. ^{1}H NMR (400 MHz, $CDCl_3$) δ 3.73 (s, 3H, OCH_3), 3.68 (s, 2H, ICH_2).

Methyl 3-iodopropionate

Using a modified Finkelstein procedure,[46] methyl 3-iodopropionate (23.10 g, 108 mmol, 90%) was prepared from methyl 3-bromopropionate (20.00 g, 120 mmol) and sodium iodide (22.98 g, 153 mmol, 1.28 eq.) in acetone (80 mL) as an orange oil. ^{1}H NMR (400 MHz, $CDCl_3$) δ 3.71 (s, 3H, OCH_3), 3.31 (s, 2H, $J = 7.2$ Hz, ICH_2), 2.97 (s, 2H, $J = 7.2$ Hz, CH_2CO_2).

Methyl cyclopenta-1,3-dienylacetate and methyl cyclopenta-1,4-dienylacetate[47,48]

A solution of methyl iodoacetate (18.50 g, 92.5 mmol) in anhydrous tetrahydrofuran (60 mL) was added dropwise to a 2.0 M solution of sodium cyclopentadienide (46.3 mL, 92.5 mmol) in tetrahydrofuran over 15 min under nitrogen at −78 °C. The

resulting reaction mixture was stirred for a further 3 h at −78 °C and then warmed to room temperature, filtered and the resulting solid was washed with diethyl ether (200 mL). The combined organics were concentrated *in vacuo*. The crude oil was purified by flash chromatography on silica using 10% ethyl acetate in *iso*-hexane to afford methyl 3-cyclopenta-1,3-dienylacetate (1-alkylCp) and methyl 3-cyclopenta-1,4-dienylacetate (2-alkylCp) (2.37 g, 17.3 mmol, 19%) as yellow liquids in an approx. 1 : 1 ratio. ^{1}H NMR (500 MHz, $CDCl_3$) δ 6.53 (m, 1H, Cp CH), 6.46 (m, 2H, Cp CH), 6.37 (m, 2H, Cp CH), 6.23 (m, 1H, Cp CH), 3.72 (s, 3H, OCH_3), 3.71 (s, 3H, OCH_3), 3.47 (m, 2H, CH_2), 3.44 (m, 2H, CH_2), 3.04 (m, 2H, CH_2), 3.02 (m, 2H, CH_2).

Methyl 3-cyclopenta-1,3-dienylpropionate and methyl 3-cyclopenta-1,4-dienylpropionate[48]

A 2.0 M solution of sodium cyclopentadienide in tetrahydrofuran (105 mL, 210 mmol) was added dropwise over 15 min to a stirred solution of methyl 3-iodopropionate (45.00 g, 210 mmol) in anhydrous diethyl ether (280 mL) and anhydrous tetrahydrofuran (200 mL) under nitrogen at −78 °C. The resulting reaction mixture was stirred at −78 °C for 2 h and then stored at −20 °C for a further 15 h. The resulting red suspension was quenched with 1 M ammonium chloride solution (800 mL), and the organic phase was extracted with diethyl ether (5 x 400 mL). The combined organic layer was washed with 1 M ammonium chloride solution (2 x 500 mL) and dried (anhydrous sodium sulfate), filtered and concentrated *in vacuo*. The crude oil was purified by flash chromatography on silica using 5% ethyl acetate in *iso*-hexane to afford methyl 3-cyclopenta-1,3-dienylpropionate (1-alkylCp) and methyl 3-cyclopenta-1,4-dienylpropionate (2-alkylCp) (14.72 g, 96.7 mmol, 46%) as yellow liquids in a 1.2 : 1 ratio. Major isomer (1-alkylCp): ^{1}H NMR (400 MHz, $CDCl_3$) δ 6.40 (m, 1H, Cp-H3), 6.25 (m, 1H, Cp-H4), 6.02 (m, 1H, Cp-H2), 3.66 (s, 3H, OCH_3), 2.93 (dd, 2H, J = 3.7 and 1.9 Hz, Cp-H5), 2.71 (m, 2H, CH_2CO_2), 2.55 (m, 2H, $CpCH_2$). Minor isomer (2-alkylCp): ^{1}H NMR (400 MHz, $CDCl_3$) δ 6.40 (m, 1H, Cp-H3), 6.39 (m, 1H, Cp-H4), 6.16 (m, 1H, Cp-H1), 3.66 (s, 3H, OCH_3), 2.88 (dd, 2H, J = 2.9 and 1.5 Hz, Cp-H5), 2.71 (m, 2H, CH_2CO_2), 2.55 (m, 2H, $CpCH_2$).

$[Fe(C_5H_4CH_2CO_2Me)(CO)_2]_2$

A mixture of methyl 3-cyclopenta-1,3-dienylacetate (1-alkylCp) and methyl 3-cyclopenta-1,4-dienylacetate (2-alkylCp) (2.00 g, 14.59 mmol) in degassed heptane (55 mL) was added to diiron nonacarbonyl (5.31 g, 14.59 mmol) under nitrogen at room temperature. The resulting reaction mixture was heated to reflux at 110 °C and stirred for 18 h, then cooled to ambient temperature at which point precipitation of maroon crystals was observed. The solution was further cooled in the freezer for 1 h and then filtered through a sinter funnel. The crystals collected were washed thoroughly with degassed hexane (4 x 50 mL). The crystals were dissolved in degassed dichloromethane (4 x 50 mL) and the solvent was concentrated *in vacuo* to yield the iron sandwich complex (2.67 g, 5.36 mmol, 30%) as maroon crystals. ^{1}H NMR (500 MHz, CD_2Cl_2, RT) δ 4.76 (br, 4H, Cp), 4.69 (br, 4H, Cp), 3.74 (s, 6H, OMe), 3.56 (s, 4H CH_2). ^{13}C NMR (126 MHz, CD_2Cl_2, −30 °C) δ 272.5 (bridging CO), 210.3 (terminal CO), 171.2 (C=O), 98.0 (Cp C), 89.7 (Cp CH), 89.4 (Cp CH), 52.5 (OCH_3), 32.4 (CH_2). IR (solid) ν(cm^{-1}) 1979 (s), 1946 (s), 1759 (s), 1737 (s).

$[Fe(C_5H_4CH_2CH_2CO_2Me)(CO)_2]_2$

Using the same procedure as for $[Fe(C_5H_4CH_2CO_2Me)(CO)_2]_2$ above, $[Fe(C_5H_4CH_2CH_2CO_2Me)(CO)_2]_2$ (12.75 g, 24.20 mmol, 50%) was prepared as maroon crystals from a mixture of methyl 3-cyclopenta-1,3-dienylpropionate and methyl 3-cyclopenta-1,4-dienylpropionate (1.2 : 1, 14.50 g, 96 mmol) and diiron nonacarbonyl (34.90 g, 96 mmol) in degassed heptane (350 mL). ^{1}H NMR (500 MHz, CD_2Cl_2, RT) δ 4.67 (s, 4H, Cp CH), 4.56 (s, 4H, Cp CH), 3.71 (s, 6H, OCH_3), 2.80 (s, 4H, CH_2), 2.66 (s, 4H, CH_2). ^{1}H NMR (500 MHz, CD_2Cl_2, −30 °C) δ 4.67 (br, 4H, Cp CH), 4.57 (br, 4H, Cp CH), 3.67 (s, 6H, OCH_3), 2.76 (s, 4H, CH_2), 2.68 (4H, CH_2). ^{1}H NMR (500 MHz, CD_2Cl_2, −50 °C) δ 4.58 (br, 8H, Cp CH), 3.65 (s, 6H, OCH_3), 2.68 (s, 8H, CH_2). ^{13}C NMR (126 MHz, CD_2Cl_2, RT) δ 172.7 (ester C=O), 105.6 (Cp C), 88.3 (Cp CH), 87.4 (Cp CH), 51.5 (2 × OCH_3), 34.3 (CH_2), 22.5 (CH_2). ^{13}C NMR (126 MHz, CD_2Cl_2, −30 °C) δ 272.9 (bridging CO), 210.8 (terminal CO), 173.1 (ester C=O), 105.2 (Cp C), 87.9 (Cp CH), 87.0 (Cp CH), 52.1 (OCH_3), 34.3 (CH_2), 22.5 (CH_2). IR (solid) ν(cm^{-1}) 1976 (s), 1937 (s), 1788 (s), 1715 (s).

$[Fe(C_5H_4CH_2CO_2Me)(CO)_3][BF_4]$

The following procedure is based on a modified literature method.[22] Ferrocinium tetrafluoroborate (274 mg, 1.00 mmol, 2 eq.) was added to $[Fe(C_5H_4CH_2CO_2Me)(CO)_2]_2$ (250 mg, 0.502 mmol) under nitrogen. An anhydrous mixture of degassed DCM–THF (33 mL; 2 : 1) was added and CO was then bubbled through the resulting reaction mixture for a period of 15 min. The reaction mixture was then stirred under a CO atmosphere. After 18 and 24 h, CO was passed through the reaction mixture for 10 min. In total, the reaction mixture was stirred under a CO atmosphere for 36 h after which the reaction flask was flushed with nitrogen. The reaction mixture was then concentrated *in vacuo* and the resulting black solid was washed with degassed diethyl ether (5 × 20 mL), after which the product was extracted with degassed DCM (5 × 20 mL). The combined organic layers were concentrated *in vacuo* to give an orange solid which was then washed with degassed dichloromethane (20 mL). The resulting yellow solid was dissolved in acetone (20 mL), filtered and the solvent removed *in vacuo* to give the title compound as a yellow solid (66.4 mg, 0.183 mmol, 36%). ^{1}H NMR (500 MHz, CD_3COCD_3, RT, low concentration sample) δ 6.25 (t, 2H, Cp CH), 6.08 (t, 2H, Cp CH), 3.87 (s, 2H, CH_2), 3.77 (s, 3H, OCH_3). ^{1}H NMR (500 MHz, CD_3COCD_3, RT, high concentration sample) δ 6.22 (br, 2H, Cp CH), 6.06 (br, 2H, Cp CH), 3.86 (s, 2H, CH_2), 3.77 (s, 3H, OCH_3). ^{13}C NMR (126 MHz, CD_3COCD_3, −30 °C) δ 204.7 (terminal CO), 170.9 (ester C=O), 106.4 (Cp C), 92.9 (Cp CH), 89.7 (Cp CH), 53.4 (OCH_3), 32.1 (CH_2). IR (solid) ν(cm^{-1}) 2121 (s), 2065 (s), 1737 (s).

$[Fe(C_5H_4CH_2CH_2CO_2Me)(CO)_3]BF_4]$

Using the ferrocinium oxidation procedure given above,[22] $[Fe(C_5H_4CH_2CH_2CO_2Me)(CO)_3][BF_4]$ (95.0 mg, 0.251 mmol, 15%) was prepared as a yellow solid from $[Fe(C_5H_4CH_2CH_2CO_2Me)(CO)_2]_2$ (900 mg, 1.71 mmol) and ferrocinium tetrafluoroborate (933 mg, 3.42 mmol, 2 eq.) under a carbon

monoxide atmosphere for 36 h. IR (solid) ν(cm^{-1}) 2059 (s), 2009 (s), 1735 (s). ^{1}H NMR (400 MHz, CD_3COCD_3, RT, low concentration sample) δ 6.15 (t, 2H, Cp CH), 6.07 (t, 2H, Cp CH), 3.67 (s, 3H, OCH_3), 2.94 (t, 2H, CH_2), 2.80 (t, 2H, CH_2, signal overlaps with H_2O signal). ^{1}H NMR (500 MHz, CD_3COCD_3, RT, high concentration sample) δ 6.13 (br, 2H, Cp CH), 6.05 (br, 2H, Cp CH), 3.67 (s, 3H, OCH_3), 2.93 (t, 2H, CH_2), 2.82 (t, 2H, CH_2). ^{13}C NMR (126 MHz, CD_3COCD_3, −30 °C) δ 203.7 (terminal CO), 172.1 (ester C=O), 114.1 (Cp C), 89.4 (Cp CH), 88.8 (Cp CH), 51.4 (OCH_3), 32.8 (CH_2), 22.2 (CH_2).

X-Ray crystallography‡

The structure determination data are summarised in Table S2§. Data collected were measured on a Bruker Smart CCD area detector with Oxford Cryosystems low temperature system. Reflections were measured from a hemisphere of data collected of frames each covering 0.3° in ω. All of the measured reflections were corrected for Lorentz and polarisation effects and for absorption by semi-empirical methods based on symmetry-equivalent and repeated reflections. The structure was solved by direct methods and refined by full matrix least squares methods on F^2. Hydrogen atoms were placed geometrically and refined with a riding model (including torsional freedom for methyl groups) and with U_{iso} constrained to be 1.2 (1.5 for methyl groups) times U_{eq} of the carrier atom. Complex scattering factors were taken from the program package SHELXTL[49] as implemented on the Viglen Pentium computer.

Cell culture and biological assays

The assays were performed following the published procedure.[50] Murine RAW264.7 macrophages were purchased from the European Collection of Cell Cultures (Salisbury, Wiltshire, UK) and cultured in Dulbecco's modified Eagle's medium (DMEM) supplemented with 10% fetal bovine serum, 2 mM L-glutamine, 100 units mL^{-1} penicillin and 0.1 mg mL^{-1} streptomycin. Cultures were maintained at 37 °C in a 5% CO_2 humidified atmosphere and experiments were conducted on cells at approximately 80–90% confluence. Macrophages were exposed for 24 h to LPS (1 μg mL^{-1}) in the presence or absence of CO-RMs (10, 50 and 100 μM) and nitrite levels and cytotoxicity were determined at the end of the incubation. Nitrite levels were determined using the Griess method as previously described.[51] The measurement of this parameter is widely accepted as indicative of NO production and inflammation. Briefly, the medium from treated cells cultured in 24 well plates was removed and placed into a 96 well plate (50 μl per well). The Griess reagent was added to each well to begin the reaction, the plate was shaken for 10 min and the absorbance read at 550 nm on a Molecular Devices VERSAmax plate reader. The nitrite level in each sample was calculated from a standard curve generated with sodium nitrite (0 μM to 300 μM in cell culture medium). Cell viability was determined using an Alamar Blue assay kit and carried out according to the manufacturer's instructions (Serotec, UK) as previously reported.[52] The assay is based on the detection of metabolic activity of living cells using a redox indicator which changes from an oxidised (blue) form to a reduced (red) form. The intensity of the red colour is proportional to the metabolism of the cells, which is calculated as the difference in absorbance between 570 nm and 600 nm and expressed as a percentage of control.

Acknowledgements

This work was supported by a EPSRC DTA studentship (DS) and PDRA (TRJ) and Hemocorm Ltd.

References

1 T. R. Johnson, B. E. Mann, J. E. Clark, R. Foresti, C. Green and R. Motterlini, *Angew. Chem., Int. Ed.*, 2003, **42**, 3722.
2 K. Sato, J. Balla, L. Otterbein, R. N. Smith, S. Brouard, Y. Lin, E. Csizmadia, J. Sevigny, S. C. Robson, G. Vercellotti, A. M. Choi, F. H. Bach and M. P. Soares, *J. Immunol.*, 2001, **166**, 4185.
3 M. Lavitrano, R. T. Smolenski, A. Musumeci, M. Maccherini, E. Slominska, E. di Florio, A. Bracco, A. Mancini, G. Stassi, M. Patti, R. Giovannoni, A. Froio, F. Simeone, M. Forni, M. L. Bacci, G. D'Alise, E. Cozzi, L. E. Otterbein, M. H. Yacoub, F. H. Bach and F. Calise, *FASEB J.*, 2004, **18**, U709.
4 L. E. Otterbein, B. S. Zuckerbraun, M. Haga, F. Liu, R. Song, A. Usheva, C. Stachulak, N. Bodyak, R. N. Smith, E. Csizmadia, S. Tyagi, Y. Akamatsu, R. J. Flavell, T. R. Billiar, E. Tzeng, F. H. Bach, A. M. K. Choi and M. P. Soares, *Nat. Med.*, 2003, **9**, 183.
5 B. S. Zuckerman, B. Y. Chin, B. Wegiel, T. R. Billiar, E. Czsimadia, J. Rao, L. Shimoda, E. Ifedigbo, S. Kanno and L. Otterbein, *J. Exp. Med.*, 2006, **203**, 2109.
6 R. Motterlini, J. E. Clark, R. Foresti, P. Sarathchandra, B. E. Mann and C. J. Green, *Circ. Res.*, 2002, **90**, 1.
7 J. E. Clark, P. Naughton, S. Shurey, C. J. Green, T. R. Johnson, B. E. Mann, R. Foresti and R. Motterlini, *Circ. Res.*, 2003, **93**, e2; T. R. Johnson, B. E. Mann, I. P. Teasdale, H. Adams, R. Foresti, C. J. Green and R. Motterlini, *Dalton Trans.*, 2007, 1500.
8 A. B. Stein, Y. R. Guo, W. Tan, W. J. Wu, X. P. Zhu, Q. H. Li, C. Luo, B. Dawn, T. R. Johnson, R. Motterlini and R. Bolli, *J. Mol. Cell. Cardiol.*, 2005, **38**, 127.
9 T. Vera, J. R. Henegar, H. A. Drummond, J. M. Rimoldi and D. E. Stec, *J. Am. Soc. Nephrol.*, 2005, **16**, 950.
10 Y. Tayem, T. R. Johnson, B. E. Mann, C. J. Green and R. Motterlini, *Am. J. Physiol.–Renal*, 2006, **290**, F789.
11 R. Motterlini, P. Sawle, J. Hammad, S. Bains, R. Alberto, R. Foresti and C. J. Green, *FASEB J.*, 2005, **19**, 284.
12 R. A. Motterlini and B. E. Mann, Preparation of metal complexes for therapeutic delivery of carbon monoxide as vasodilator, *PCT Int. Appl.*, WO 0292075 A2 20021121. Granted in US, US7045140, 2002; R. A. Motterlini, B. E. Mann, T. R. Johnson, D. A. Scapens and R. Aqil, Therapeutic deliveryof carbon monoxide via organometallic complexes, *PCT Int. Appl.*, WO 2007085806 A2 20070802, 2007.
13 I. J. S. Fairlamb, A. K. Duhme-Klair, J. M. Lynam, B. E. Moulton, C. T. O'Brien, P. Sawle, J. Hammad and R. Motterlini, *Bioorg. Med. Chem. Lett.*, 2005, **16**, 995; P. Sawle, J. Hammad, I. J. S. Fairlamb, B. Moulton, C. T. O'Brien, J. M. Lynam, A. K. Duhme-Klair, R. Foresti and R. Motterlini, *J. Pharmacol. Exp. Ther.*, 2006, **318**, 403.
14 R. C. Kerber, *Comprehensive Organometallic Chemistry II*, ed. D. F. Shriver and M. I. Bruce, 1995, vol. 7, ch. 2.
15 W. A. G. Graham and W. Jetz, *Inorg. Chem.*, 1971, **10**, 1159.
16 Y. Fu, P. Chao and L. Liu, *Organometallics*, 1998, **17**, 221.
17 J. Ellermann, H. Behrens and H. Krohberger, *J. Organomet. Chem.*, 1972, **46**, 119.
18 E. Weiss, R. Merenyi, W. Huebel, J. Nielsen, A. Gerondal and R. Vannieuwenhoven, *Chem. Ber.*, 1962, **95**, 1170.
19 N. J. Coville, K. E. du Plooy and W. Pickl, *Coord. Chem. Rev.*, 1992, **116**, 1.
20 N. J. Coville, M. S. Loonat, D. White and L. Carlton, *Organometallics*, 1992, **11**, 1082.
21 M. M. Singh and R. J. Angelici, *Inorg. Synth.*, 1986, **24**, 161.
22 D. Catheline and D. Astruc, *Organometallics*, 1984, **3**, 1094.
23 A. R. Manning, G. McNally, D. Cunningham, P. McArdle and J. M. Simmie, *J. Organomet. Chem.*, 1988, **388**, 383.
24 N. Xiao, B. Wang, J. Yin, Q. Xu, N. Tsumori, J. Sun and J. Chen, *Organometallics*, 2004, **23**, 257; O. S. Mills, *Acta Crystallogr.*, 1958, **11**, 620; R. F. Bryan, P. T. Greene, M. J. Newlands and D. S. Field, *J. Chem. Soc. A*, 1970, 3064; A. Mitschler, B. Rees and M. S. Lehmann, *J. Am. Chem. Soc.*, 1978, **100**, 3390; A. S. Batsanov, B. M. Bridgewater, J. A. K. Howard, A. K. Hughes and C. Wilson, *J. Organomet. Chem.*, 1999, **590**, 169; B. Wang, B. Zhu, J. Zhang, S. Xu, X. Zhou and

L. Weng, *Organometallics*, 2003, **22**, 5543; R. G. Teller and J. M. Williams, *Inorg. Chem.*, 1980, **19**, 2770; M. Enders, P. Fernandez, M. Kaschke, G. Kohl, G. Ludwig, H. Pritzkow and R. Rudolph, *J. Organomet. Chem.*, 2002, **641**, 81; L. P. Barthel-Rosa, J. R. Sowa Jr, P. G. Gassman, J. Fischer, B. M. McCarty, S. L. Goldsmith, M. T. Gibson and J. H. Nelson, *Organometallics*, 1997, **16**, 1595; P. McArdle, L. O'Neill and D. Cunningham, *Organometallics*, 1997, **16**, 1335; F. A. Cotton, B. A. Frenz, J. M. Troup and G. deGanello, *J. Organomet. Chem.*, 1973, **59**, 317; H.-L. Sun, X.-Z. Zhou, X.-K. Yao and H.-G. Wang, *Polyhedron*, 1996, **15**, 4489; D. Chen, Y. Li, B. Wang, S. Xu and H. Song, *Organometallics*, 2006, **25**, 307; J. D. Cotton, K. A. Byriel, C. H. L. Kennard, T. Scheck and D. E. Lynch, *J. Organomet. Chem.*, 1993, **462**, 243; N. H. T. Huy, L. Ricard and F. Mathey, *Organometallics*, 1995, **14**, 4048.

25 M. Scheer, K. Schuster, U. Becker, A. Krug and H. Hartung, *J. Organomet. Chem.*, 1993, **460**, 105.

26 R. F. Bryan, P. T. Greene, M. J. Newlands and D. S. Field, *J. Chem. Soc. A*, 1970, 3068; J. M. Burlitch, J. H. Burk, M. E. Leonoxicz and R. Hughes, *Inorg. Chem.*, 1979, **18**, 1702; L. A. Paquette, J. A. McKinney, M. L. Laughlin and A. L. Rheingold, *Tetrahedron Lett.*, 1986, **27**, 5599; N. E. Kim, N. J. Nelson and D. F. Shriver, *Inorg. Chim. Acta*, 1973, **7**, 393; H. Hu, G. Nie, Z. Jin and W. Chen, *J. Organomet. Chem.*, 1989, **377**, 137; J. D. Cotton, K. A. Byriel, C. H. L. Kennard, T. Scheck and D. E. Lynch, *J. Organomet. Chem.*, 1993, **462**, 243; X. He, R. A. Bartlett and P. P. Powell, *Organometallics*, 1994, **13**, 548.

27 K.-J. Jens and E. Weiss, *Acta Crystallogr., Sect. C: Cryst. Struct. Commun.*, 1985, **41**, 895.

28 W. Clegg, N. A. Compton, R. J. Errington and N. C. Norman, *J. Chem. Soc., Dalton Trans.*, 1988, 1671.

29 L. D. Field, T. W. Hambley, C. M. Lindall and A. F. Masters, *Polyhedron*, 1989, **8**, 2425.

30 V. W. Day, M. R. Thompson, G. O. Nelson and M. E. Wright, *Organometallics*, 1983, **2**, 494; P. McArdle, L. O'Neill and D. Cunningham, *Inorg. Chim. Acta*, 1999, **291**, 252; Y. Zhang, B. Wang, S. Xu and X. Zhou, *Transition Met. Chem.*, 1999, **24**, 722; H. Sun, Z. Zhang, Y. Pan, J. Yang and X. Zhou, *Inorg. Chem.*, 2003, **42**, 4076; T. Yu, Orlova, V. N. Setkina, P. V. Petrovskii, A. I. Yanovsky, A. S. Batsanov and Yu. T. Struchkov, *Metallurg. Khim.*, 1988, **1**, 1327; C. I. Sterzo, M. M. Miller and J. K. Stille, *Organometallics*, 1989, **8**, 2331; S.-S. Xu, X.-B. Zhong and X.-Z. Zhou, *Huaxue Xuebao*, 1996, **54**, 1209; C.-H. Kong, S.-S. Xu and X.-Z. Zhou, *Huaxue Xuebao*, 1995, **53**, 816.

31 T. Katayama, Y. Morimoto, M. Yuge, M. Uno and S. Takahashi, *Organometallics*, 1999, **18**, 3087.

32 M. Zeller, E. Lazich and A. D. Hunter, *Acta Crystallogr., Sect. E: Struct. Rep. Online*, 2003, **E59**, m914.

33 D. I. Coombs, S. Aldridge, A. Rossin, C. Jones and D. J. Willock, *Organometallics*, 2004, **23**, 2911.

34 Yu. T. Struchkov, G. G. Aleksandrov, V. S. Kaganovich and M. I. Rubinskaya, *Koord. Khim.*, 1981, **7**, 949.

35 M. E. Gress and R. A. Jacobson, *Inorg. Chem.*, 1973, **12**, 1746; S. Aldridge, R. J. Calder, S. J. Coles and M. B. Hursthouse, *J. Chem. Crystallogr.*, 2003, **33**, 805; S. Du, J. A. Kautz, T. D. McGrath and F. G. A. Stone, *Dalton Trans.*, 2003, 46; N. R. Bunn, S. Aldridge, D. L. Kays, N. D. Coombs, J. K. Day, L.-l. Ooi, S. J. Coles and M. B. Hursthouse, *Organometallics*, 2005, **24**, 5879; P. McArdle, D. MacHale, D. Cunningham and A. R. Manning, *J. Organomet. Chem.*, 1991, **419**, C18; P. Roussel, D. R. Cary, S. Barlow, J. C. Green, F. Varret and D. O'Hare, *Organometallics*, 2000, **19**, 1071; I. Emme, T. Labahn and A. de Meijere, *Eur. J. Org. Chem.*, 2006, 399; K. A. Pevear, M. M. B. Holl, G. B. Carpenter, A. L. Reiger, P. H. Reiger and D. A. Sweigart, *Organometallics*, 1995, **14**, 512; X. Solans and M. Font-Bardia, *Acta Crystallogr., Sect. C: Cryst. Struct. Commun.*, 1995, **C51**, 2255.

36 L. F. Dahl, R. J. Doedens, W. Hubel and J. Nielsen, *J. Am. Chem. Soc.*, 1966, **88**, 446; Y. Morimoto, K. Ando, M. Uno and S. Takahashi, *Chem. Commun.*, 1997, 1795.

37 H.-H. Gau, C.-C. Schei, L.-K. Liu and L.-H. Luh, *J. Organomet. Chem.*, 1992, **435**, 43.

38 M. D. Bala, A. Munyaneza and N. J. Coville, *Acta Crystallogr., Sect. E: Struct. Rep. Online*, 2005, **E61**, m2124.

39 A. R. Manning, *J. Chem. Soc. A*, 1968, 1319.

40 M. A. Guillevic, E. L. Hancox and B. E. Mann, *J. Chem. Soc., Dalton Trans.*, 1992, 1729.

41 J. A. Bullitt, F. A. Cotton and T. J. Marks, *J. Am. Chem. Soc.*, 1970, **92**, 3155; R. D. Adams and F. A. Cotton, *J. Am. Chem. Soc.*, 1973, **95**, 6589; O. A. Gansow, A. R. Burke and W. D. Vernon, *J. Am. Chem. Soc.*, 1976, **98**, 5817.

42 M. A. Guillevic, E. L. Hancox and B. E. Mann, *J. Chem. Soc., Dalton Trans.*, 1992, 1729.

43 E. H. Braye and W. Hübel, *Inorg. Synth.*, 1966, **8**, 178.

44 T. S. Piper, F. A. Cotton and G. Wilkinson, *J. Inorg. Nucl. Chem.*, 1955, **1**, 165; T. S. Piper and G. Wilkinson, *J. Inorg. Nucl. Chem.*, 1956, **2**, 38; R. B. King and M. B. Bisnette, *J. Am. Chem. Soc.*, 1964, **86**, 1267; C. E. Coffey, *J. Inorg. Nucl. Chem.*, 1963, **25**, 179.

45 G. L. Grunewald and D. P. Davis, *J. Org. Chem.*, 1978, **43**, 3074.

46 E. S. Hand, S. C. Johnson and D. C. Baker, *J. Org. Chem.*, 1997, **62**, 1348.

47 P.-H. Yeh, Z. Pang and R. F. Johnston, *J. Organomet. Chem.*, 1996, **509**, 123.

48 R. A. L. Gendron, D. J. Berg and T. Barclay, *Can. J. Chem.*, 2002, **80**, 1285.

49 *SHELXTL version, An integrated system for solving and refining crystal structures from diffraction data (Revision 5.1)*, Bruker AXS Ltd.

50 P. Sawle, R. Foresti, B. E. Mann, T. R. Johnson, C. J. Green and R. Motterlini, *Br. J. Pharmacol.*, 2005, **145**, 800.

51 R. Foresti, J. E. Clark, C. J. Green and R. Motterlini, *J. Biol. Chem.*, 1997, **272**, 18411.

52 J. E. Clark, R. Foresti, C. J. Green and R. Motterlini, *Biochem. J.*, 2000, **348**, 615.